Dalton Transactions

PAPER

View Article Online
View Journal | View Issue

Cite this: *Dalton Trans.*, 2016, **45**, 17910

Spin-state diversity in a series of Co(II) PNP pincer bromide complexes†

David W. Shaffer,‡§[c] Indrani Bhowmick,§[a] Arnold L. Rheingold,[b] Charlene Tsay,[c] Brooke N. Livesay,[a,c] Matthew P. Shores*[a] and Jenny Y. Yang*[c]

Received 5th September 2016,
Accepted 13th October 2016

DOI: 10.1039/c6dt03461f

www.rsc.org/dalton

We describe the structural and electronic impacts of modifying the bridging atom in a family of Co(II) pincer complexes with the formula Co(*t*-Bu)$_2$P^{E}Py^{E}P(*t*-Bu)$_2$Br$_2$ (Py = pyridine, E = CH_2, NH, and O for compounds **1–3**, respectively). Structural characterization by single crystal X-ray diffraction indicates that compounds **1** and **3** are 5-coordinate complexes with both bromides bound to the Co(II) ion, while compound **2** is square planar with one bromide in the outer coordination sphere. The reduction potentials of **1–3**, characterized by cyclic voltammetry, are consistent with the increasing electron-withdrawing character of the pincer ligand as the linker (E) between the pyridine and phosphine arms becomes more electronegative. Magnetic property studies of compounds **1** and **2** confirm high- and low-spin behavior, respectively, through a broad temperature range. However, complex **3** features an unusual combination of high spin S = 3/2 Co(II) and temperature dependent spin-crossover between S = 3/2 and S = 1/2 states. The different magnetic behaviors observed among the three $CoBr_2$ pincer complexes reflects the importance of small ligand perturbations on overall coordination geometry and resulting spin state properties.

Introduction

The electronic ground states enforced by the coordination environment in transition metal complexes define their magnetic properties and chemical behavior. Weak field ligand environments that promote high-spin states often result in greater metal complex reactivity in atom or group transfer reactions.[1–7] Intermediate ligand field environments can generate transition metal complexes that have temperature-dependent changes between low- and high- spin states. These compounds attract a great deal of interest for their fundamental magnetic properties and potential application in switchable materials.[8,9] They are also known to possess unique reactivity.[10,11]

The spin-crossover/transition phenomenon provides an externally accessible link between magnetic, optical, vibrational, structural, and thermodynamic properties for inorganic coordination complexes.[12] Spin state switching properties can be influenced by very small changes in coordination environment and/or supramolecular interactions. Although the majority of known spin-crossover compounds contain Fe(II) and Fe(III) ions,[13–16] Co(II) complexes in 4-, 5-, or 6-coordinate environments can also exhibit spin-crossover/transition behavior between the high-spin S = 3/2 and low-spin S = 1/2 states.[17–21] Sacconi showed that the magnetic spin crossover of 5-coordinate Co(II) complexes depends not only on the D_q values (donor strength), but also on the electron delocalization onto the ligand.[22] To investigate how small changes in the ligand environment can influence the spin state of a Co(II) ion, we have prepared, structurally characterized, and measured the electronic and magnetic properties of $CoBr_2$ complexes of the tridentate pincer ligands (P^{E}N^{E}P), shown in Chart 1. The bromide derivative was investigated because prior studies on Co(II) complexes with tridentate ligands indicate that bromide coordination is most likely to result in favorable

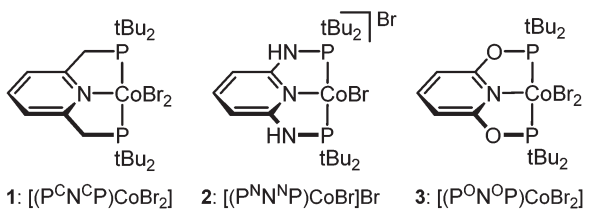

1: [(P^{C}N^{C}P)CoBr$_2$] **2**: [(P^{N}N^{N}P)CoBr]Br **3**: [(P^{O}N^{O}P)CoBr$_2$]

Chart 1

[a]*Department of Chemistry, Colorado State University, Fort Collins, CO 90523, USA*
[b]*Department of Chemistry and Biochemistry, University of California, San Diego, La Jolla, CA 92093, USA*
[c]*Department of Chemistry, University of California, Irvine, Irvine, CA 92697, USA. E-mail: j.yang@uci.edu*

†Electronic supplementary information (ESI) available: X-ray diffraction and refinement parameters, ^{1}H NMR, magnetic data, and modelling. CCDC **1** 1022626–1022628 for **1**, **2** and **3**. For ESI and crystallographic data in CIF or other electronic format see DOI: 10.1039/c6dt03461f

‡Current address: Chemistry Division, Brookhaven National Laboratory, Upton, NY 11973, USA.
§These authors contributed equally to this work.

spin-transition properties at the Co(II) center,[23,24] whereas the chloride and iodide analogues are mostly high- and low-spin, respectively.[22,24]

Cobalt complexes with these ligands are currently of interest because of their reactivity and catalytic properties.[25–28] The use of atomic linkers of increasing electronegativity (E = CH_2, NH, O) between the phosphine arms and pyridine generates a stepwise increase in the electron withdrawing nature of the ligand[29] without significantly impacting other structural parameters. The related 5-coordinate Co(II)LBr_2 pincer complexes (L = PNP, PNN) have shown spin state switching properties,[17–24,30] but the extent to which Co(II) spin states can be tuned by substitution at the non-coordinated atom(s) of PNP-type ligands has not been investigated systematically. This study describes how ligand perturbations affect the coordination geometry and corresponding electronic structure, which is critical in evaluating the propensity of ligand modifications to fine-tune physical properties and tailor reactivity.

Results and discussion

Synthesis, characterization, and structural studies of $(P^ENE^P)CoBr_2$ (1–3)

The bis(phosphino)pyridine compounds P^CN^CP, P^NN^NP, P^ON^OP shown in Chart 1 were synthesized according to literature preparations.[31–33] Dichloromethane solutions of the P^EN^EP (E = C, N, O) ligands were added to $CoBr_2$ dissolved in acetonitrile to give the complexes $(P^EN^EP)CoBr_2$ (E = C, **1**; O, **3**) or $[(P^NN^NP)CoBr]Br$ (**2**). The dark purple crude product of **1** was isolated by solvent removal and recrystallized by layering pentane over a saturated dichloromethane solution to give the analytically pure product in 96% yield. Related preparations have been reported for other $(P^CN^CP)CoX_2$ (X = Cl, Br, I) complexes.[24,27,34–36] Product **2** precipitated from the reaction solution and was isolated in 92% yield after washing with diethyl ether. The dark violet crude product for $(P^ON^OP)CoBr_2$ (**3**) was isolated by solvent removal and recrystallized by layering dichloromethane solutions with pentane to give the product in up to 31% yield. Compounds **1** and **3** are soluble in polar organic solvents such as dichloromethane and acetonitrile; in contrast **2** has limited solubility, even in alcoholic solvents, reflecting the different coordination geometry of the three dibromide complexes (*vide infra*). The identity and purity of **1**, **2**, and **3** were determined by X-ray crystallography, ESI-MS, and elemental analyses.

Single-crystal X-ray diffraction analysis of **1** revealed a 5-coordinate cobalt(II) center with a geometry between square pyramidal and trigonal bipyramidal, shown in Fig. 1a. Selected metrical parameters are provided in Table 1. The asymmetric unit contains two molecules of **1** and one molecule of CH_2Cl_2. In both molecules of **1**, the largest angle around the cobalt center is between the pyridine donor and the bromide approximately *trans* to it (N_{py}–Co–Br_{eq} = 166.25(5)° and 168.48(5)°). The P–Co–P angles are the second-largest at 140.14(2)° and 134.61(2)° in the two molecules. These values correspond to geometries close to half-way between square pyramidal and trigonal bipyramidal. The metric τ_5 can be used to describe 5-coordinate geometries in terms of their deviation from these two ideal cases, with τ_5 = 0 corresponding to square pyramidal and τ_5 = 1 corresponding to trigonal bipyramidal.[37] τ_5 is defined as the value of $(\beta - \alpha)/60$, where β is the largest ligand-metal–ligand bond angle and α is the second-largest. The values of τ_5 for the two molecules of **1** in the asymmetric unit are 0.44 and 0.56 ($\Delta\tau_5$ = 0.12). It is also notable that the pincer 'arms' are significantly twisted from the pyridine plane, with P–C–C–N torsion angles of 23.7°, 30.1°, −36.2°, and 29.4°.

X-ray diffraction analysis was performed on crystals of **2** grown by cooling a saturated EtOH solution. The single crystal X-ray structure revealed **2** to be a 4-coordinate cobalt(II) complex with an outer-sphere bromide ion in $[(P^NN^NP)CoBr]Br$. The unit cell contains eight ion pairs with the formula $[(P^NN^NP)CoBr]Br$ and eight ethanol molecules, which were highly disordered (see ESI† for more details). One of the two 4-coordinate cobalt complexes contained in the asymmetric unit is depicted in Fig. 1b with two neighboring bromide ions,

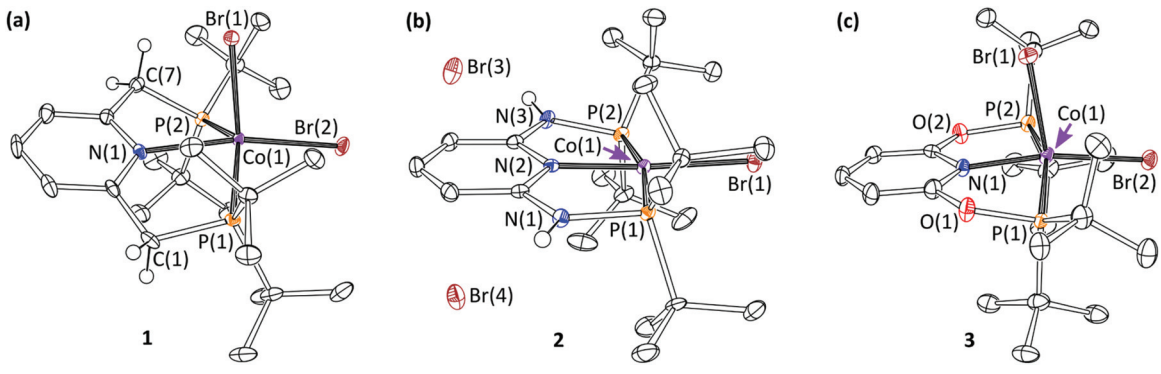

Fig. 1 (a) ORTEP of molecule A in the asymmetric unit of $(P^CN^CP)CoBr_2$ (**1**). Hydrogen atoms (except $-CH_2-$) and one molecule of CH_2Cl_2 have been omitted for clarity. (b) ORTEP of molecule A and neighboring outer-sphere bromides in the asymmetric unit of $[(P^NN^NP)CoBr]Br$ (**2**). Hydrogen atoms (except for N–H) and an ethanol molecule have been omitted for clarity. (c) ORTEP of molecule A in the asymmetric unit of $(P^ON^OP)CoBr_2$ (**3**). Hydrogen atoms have been omitted for clarity. All ellipsoids are shown at 50% probability.

Table 1 Compounds **1**, **2**, and **3** each contain two cobalt molecules in the asymmetric unit. Selected bond distances (Å) and angles (°) for both molecules and τ_5 (where relevant) for [(P^EN^EP)$CoBr_2$] (E = C, **1**; O, **3**), and [(P^NN^NP)CoBr]Br (**2**). Br_{eq} and Br_{ax} indicate the bromide ligands best described as *trans* and *cis*, respectively, from the pyridine donor

	1		**2**		**3**	
	Molecule A	Molecule B	Molecule A	Molecule B	Molecule A	Molecule B
Co–N_{py}	2.252(2)	2.270(2)	1.929(2)	1.925(2)	1.945(2)	2.134(2)
Co–$P_{1/3}$	2.4755(7)	2.4875(7)	2.2267(7)	2.2351(7)	2.2552(8)	2.4517(8)
Co–$P_{2/4}$	2.4543(7)	2.4508(7)	2.2291(7)	2.2252(8)	2.2751(8)	2.4610(9)
Co–Br_{eq}	2.4591(4)	2.4561(4)	2.3424(4)	2.3366(4)	2.3784(5)	2.4454(5)
Co–Br_{ax}	2.4576(4)	2.4713(4)	—	—	2.5930(5)	2.4333(5)
N_{py}–Co–Br_{eq}	166.25(5)	168.48(5)	175.73(6)	177.97(6)	168.83(7)	147.30(6)
P–Co–P	140.14(2)	134.61	168.48(3)	169.29(3)	156.66(3)	152.28(3)
τ_5	0.44	0.56	—	—	0.20	0.08

and selected metrical parameters are listed in Table 1. The cobalt centers in **2** are nearly square planar, with P–Co–P and N–Co–Br angles of at least 168° and the angles around the cobalt centers summing to 360.3° and 360.1°. The P–N–C–N torsion angles range from 2.55° to 12.49°, showing higher rigidity compared to the methylene 'arms' of the P^CN^CP ligand in **1**. The outer-sphere bromide ions reside between the N–H functionalities of two adjacent cobalt complexes with N···Br distances of 3.362(2), 3.426(2), 3.390(2), 3.402(2) Å, consistent with weak hydrogen bonding interactions, which likely contributes to the stability of the 4-coordinate cation.

Dark purple X-ray quality crystals of **3** were grown from dichloromethane layered with pentane. The asymmetric unit contains two 5-coordinate (P^ON^OP)$CoBr_2$ molecules, each with slightly different molecular geometries and different bond distances around the cobalt center. The structure of molecule A is shown in Fig. 1c, and the structure of molecule B is shown in Fig. S1.† Both molecules are distorted from ideal square pyramidal geometry, with the P–Co–P and N_{py}–Co–Br_{eq} angles ranging from 147° to 169°. The τ_5 parameters for the two molecules are 0.20 and 0.08 ($\Delta\tau_5$ = 0.12). These values are more consistent with distorted square pyramidal structures than trigonal bipyramidal. The more rigid arms of the P^ON^OP ligand, relative to P^CN^CP, are demonstrated by the smaller P–O–C–N torsion angles: −15.3°, −8.6°, 10.9°, and 0.1°. There is a discrepancy between the two molecules comprising the asymmetric unit. The pseudo-equatorial cobalt–ligand distances are all longer in the molecule containing Co(2) (molecule B) than those in the molecule containing Co(1) (molecule A), with a difference of approximately 0.19 Å for the neutral donors (N and P) and 0.07 Å for the bromide. On the other hand, the pseudo-axial Co–Br distance is 0.16 Å shorter in molecule B. The P–Co–P and N_{py}–Co–Br_{eq} angles of molecule B are also more acute and more similar to one another than those in molecule A, leading to a smaller value of τ. Thus, the two molecules can both be described as pseudo-square-pyramidal, with the cobalt center of molecule B being significantly more distorted towards the pseudo-axial ligand. Notably, while the Co(2)–ligand distances are generally similar to those in 5-coordinate **1**, the equatorial Co(1)–ligand distances are similar to those in 4-coordinate **2**, with the addition of a long axial Co(1)–Br bond. We attribute the distortional differences in molecule A and B to packing interactions in the solid state,[38] and the axial distortions may be associated with different spin-state behavior (*vide infra*).[22]

Electrochemical studies of (P^EN^EP)$CoBr_2$ (1–3)

The redox behavior of (P^EN^EP)$CoBr_2$ (**1–3**) was investigated by cyclic voltammetry in acetonitrile to evaluate the electronic effects of the different linkers on the ligand arms. Reduction potentials *vs.* $Fe(Cp)_2^{+/0}$ (Cp = $C_5H_5^-$) are listed in Table 2. Complexes **1–3** each exhibit two reductions as shown in Fig. 2. An additional reductive process is observed for **1** at −2.83 V. As expected, the first two reduction events shift to more positive potentials as the ligand becomes more electron-withdrawing. Based on our prior study of the corresponding [Co(P^EN^EP)$(CH_3CN)_2$]$^{2+}$ complexes, we believe the first reduction occurs

Table 2 Potentials *vs.* $Fe(Cp)_2^{+/0}$ (V) for the first (red1) and second (red2) reductions of (P^EN^EP)$CoBr_2$ complexes, (E = C, **1**; N, **2**; O, **3**), measured at 100 mV s^{-1}

Compound	E_{pc}(red2)	E_{pc}(red1′)	E_{pc}(red1)	E_{pa}(red1)
1	−2.45	−1.27[a]	−1.14	−1.05
2	−2.60	−1.22	−1.04	−0.94
3	−2.27	−0.94	—	−0.62

[a] Measured at 1600 mV s^{-1}.

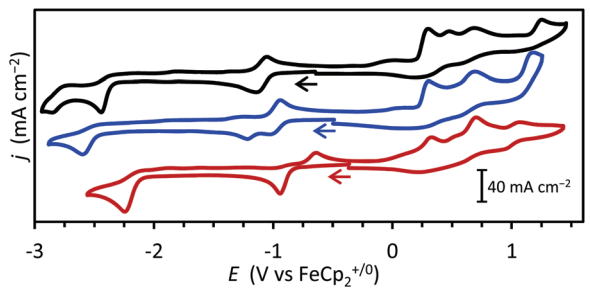

Fig. 2 Cyclic voltammograms of (P^EN^EP)$CoBr_2$ (E = C, **1**, top, black; N, **2**, middle, blue; O, **3**, bottom, red); 1.0 mM analyte in CH_3CN with 0.20 M Bu_4NPF_6 at 100 mV s^{-1}. Arrows indicate scan direction and resting potential.

at the metal.[29] We cannot definitively assign whether the additional reductive events occur on the metal or ligand because of the possibility of ligand-centered reduction.[39,40]

Cyclic voltammograms of the first reductions of **1** and **2** display scan rate dependent reversibility, shown in Fig. 3 (normalized for the diffusion controlled current at the planar electrode (current (i) $\propto \nu^{1/2}$, ν = scan rate)). At a scan rate of 25 mV s^{-1} (shown as dark red CV for **1** in Fig. 3, top), the first reduction of **1** is reversible with $E_{1/2}$ = −1.10 V. As the scan rate increases, the cathodic portion of the wave at −1.14 V (E_{pc}(red1)) decreases in intensity as another cathodic feature grows in at −1.27 V (E_{pc}(red1′)). The anodic portion of the wave remains constant (E_{pa}(red1)). Similar behavior is observed with **2**, though the second part of the feature is more evident at slower scan rates and it appears nearly irreversible at 1.6 V s^{-1} (Fig. 3, middle). As shown in Fig. 3 (bottom), **3** exhibits no partial reversibility at scan rates as low as 25 mV s^{-1}. This behavior is consistent with bromide anion dissociation upon reduction of **1**, and supported by the electrochemical behavior of the corresponding $[Co(P^CN^CP)(CH_3CN)_2]^{2+}$ complex, where the Co(II/I) redox event is reversible at all scan rates.[29] The second cathodic waves for all three dibromide complexes (and third for **1**) coincide with those of the corresponding $[(P^EN^EP)Co(CH_3CN)_2]^{2+}$ complexes, suggesting the loss of both bromide ligands occurs after the first reduction of **1–3**.[29] Furthermore, the potential of the anodic portions of the first reductions for **1–3** match closely with those for $[(P^EN^EP)Co(CH_3CN)_2]^{2+}$. After a 1-electron reduction to cobalt(I) and bromide loss, the resulting solvent adduct with the more π-accepting acetonitrile ligand $[(P^EN^EP)Co(CH_3CN)]^+$ generates the square-planar d^8 complex. Along with the 4-coordinate nature of **2** in the solid state, this suggests only a single bromide ligand remains bound to the complexes in the cobalt(II) state in polar solvents, which is exchanged for an acetonitrile upon reduction. For **1** and **2**, an equilibrium between the cobalt(II)–bromide (E_{pc} = −1.27 and −1.22 V, respectively) and the corresponding cobalt(II)–acetonitrile ($E_{1/2}$ = −1.10 and −0.96, respectively) results in the scan rate dependent observation of one or both of these species on the cathodic scan. This equilibrium is not observed for the more electron-poor **3**.

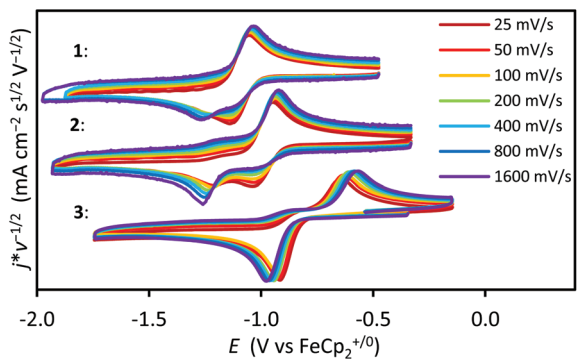

Fig. 3 Normalized cyclic voltammograms showing the first reduction events for $(P^EN^EP)CoBr_2$ (E = C, 1, top; N, 2, middle; O, 3, bottom) with varying scan rates (ν). 1.0 mM analyte in CH_3CN with 0.20 M Bu_4NPF_6.

The oxidative portions of the cyclic voltammograms for **1–3** contain a number of irreversible anodic waves, listed in Table S2.† These include a group of two to three features between 0.33 and 0.75 V, and another feature above 1 V, but were not studied further.

Solution magnetic properties of $(P^EN^EP)CoBr_2$ (1–3)

The spin states of complexes **1–3** were initially determined by EPR spectroscopy in ethanol glass at 77 K, shown in Fig. 4, and are indicative of low-spin, S = 1/2; systems. The three compounds exhibit similar spectra with signals centered around g = 2.3 and approximately 90 G hyperfine coupling to the cobalt center (I = 7/2). This indicates similar coordination environments for the Co(II) ions in the frozen ethanol solution.

At room temperature and in the aprotic solvent environment provided by chloroform, complexes **1** and **3** give solution μ_{eff} values of 4.6 and 3.9, respectively, as determined *via* Evans method (see Fig. S2†). (The low solubility of **2** in $CDCl_3$ precludes its measurement in that solvent.) These effective magnetic moment values are consistent with at least some population of high-spin states for the Co(II) ions.

From the combination of available EPR and ^{1}H NMR spectral data in ethanol and chloroform, respectively, we cannot differentiate spin-state (switching) behavior from ligand dissociation processes. The scan rate dependent cyclic voltammograms obtained in acetonitrile indicate the bromide anions are labile. The main positive ion peaks in the mass spectra acquired in acetonitrile are consistent with dissociation of one bromide for all three compounds, but this does not necessarily correspond to the speciation of neutral entities in solution. However, previous work with a series of phenyl-substituted $(P^CN^CP)CoX_2$ complexes presented evidence for both dissociation in solution and temperature-dependent spin state switching.[24] Regardless of the dominant coordination environment in solution, it is clear the variable coordination geometries and intermediate ligand fields observed for this family of complexes signified interesting spin behavior that merited further investigation.

Solid state magnetic property studies

To probe magnetic properties in an environment where more robust magnetostructural correlations can be established,

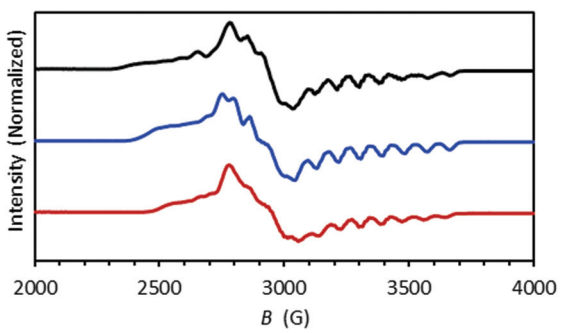

Fig. 4 EPR spectra for $(P^EN^EP)CoBr_2$ (E = C, **1**, top, black; N, **2**, middle, blue; O, **3**, bottom, red), obtained in ethanol at 77 K.

solid state magnetic properties of the complexes were studied by SQUID magnetometry (Fig. 5 and S3–S5†). As we measured crystalline samples, our data interpretation uses the chemical formulas of the solvated compounds determined from single-crystal X-ray diffraction experiments: **1**·0.25CH_2Cl_2, **2**·EtOH and **3**, respectively. At room temperature (300 K), compounds **1**·0.25CH_2Cl_2 and **3** show behavior consistent with high-spin Co(II) ions. At 300 K the $\chi_M T$ products are 2.68 and 2.78 cm^3 K mol^{-1}, respectively. These values are higher than the theoretical Curie constant for a S = 3/2 ion with g = 2 (1.875 cm^3 K mol^{-1}), but consistent with high-spin Co(II) complexes featuring significant orbital contributions: calculated room temperature g values of 2.39 and 2.44 are similar to literature values.[41,42] In contrast, the room-temperature $\chi_M T$ value for **2**·EtOH, 0.86 cm^3 K mol^{-1}, is too small to correspond to high-spin Co(II), but is consistent with a low-spin S = 1/2 Co(II) ion (theoretical Curie Constant = 0.375 cm^3 K mol^{-1}, for S = 1/2 spin with g = 2). Here, the calculated isotropic g value is large (3.02) but this is comparable with literature values.[43–45] We note that there are few examples of high-spin square planar Co(II) complexes, and they require significant electron-withdrawing capacity in ligand substituents.[46]

As the temperature is decreased, the $\chi_M T$ products for compounds **1**·0.25CH_2Cl_2 and **2**·EtOH change as expected for their respective spin states. For **1**·0.25CH_2Cl_2 the $\chi_M T$ product remains mostly constant until 70 K, and then gradually decreases to 1.52 cm^3 K mol^{-1} at 1.8 K. This temperature-dependent downturn of the $\chi_M T$ product is a signature of magnetic anisotropy related to the high-spin Co(II) centers, and/or antiferromagnetic interactions between the magnetic centers in the crystal lattice. In this regard, we note that the minimum Co–Co distances are 8.81(1) Å, 7.79(1) Å and 8.93(4) Å for **1**·0.25CH_2Cl_2, **2**·EtOH and **3**, respectively, suggesting that intermolecular antiferromagnetic interactions will be weak.

The $\chi_M T$ *vs.* T data of **1**·0.25CH_2Cl_2 are fit with program PHI,[47] using the spin Hamiltonian $\hat{H} = \mu_B g \hat{B} \hat{S} + (D/3)\hat{O}_2^0 + E\hat{O}_2^2$, where $\hat{O}$ is the Stevens operator. The best fit (Fig. 5) gives g_x = g_y = 2.385(0), g_z = 2.366(4), D = −22.324(2) cm^{-1}, E = 2.404(2) cm^{-1} and $|E/D|$ = 0.108. The magnitude of axial anisotropy $|D|$ = 22.324(2) cm^{-1} is comparable with other anisotropic 5-coordinate Co(II) complexes described in the literature;[48,49] we note that the sign of the D parameter cannot be reliably extracted from bulk magnetic measurements. As our present work is focused on spin states of the Co(II) complexes, we will not discuss further the possible dynamics of slow relaxation of magnetization of these compounds; although we note that the strong axial anisotropy of the Co(II) ion in compound **1**·0.25CH_2Cl_2 could lead to single-molecule magnet behavior.[50]

For compound **2**·EtOH, the $\chi_M T$ value preserves the paramagnet type behavior within the measured temperature range and reaches 0.81 cm^3 K mol^{-1} at 1.8 K. When the fit of the $\chi_M T$ *vs.* T data for **2**·EtOH is performed (Fig. 5), considering only an isotropic g-factor and spin Hamiltonian $\hat{H} = \mu_B g \hat{B} \hat{S}$, g_{iso} = 3.02(2) is extracted.

In contrast, the temperature dependence of $\chi_M T$ for **3** is very different from **1**·0.25CH_2Cl_2: with lowering of temperature, the $\chi_M T$ value decreases slowly until 200 K; then, between 200 K and 50 K, a comparatively steep decrease of $\chi_M T$ values is observed, consistent with spin-crossover behavior. Between 50 K and 20 K the slope of the $\chi_M T$ product is less steep, whereas below 20 K the value again decreases rapidly to 1.43 cm^3 K mol^{-1} (at 1.8 K). The lowest temperature downturn could be due to magnetic anisotropy related to any remaining high spin Co(II) centers, and/or intermolecular antiferromagnetic interactions between the Co(II) complexes. The possibility of spin transition of the Co(II) ion in **3** from S = 3/2 to S = 1/2 is known for similar 5-coordinate systems depending on the ligand field of Co(II).[18,22–24,51–53] Nelson and Kelly reported a doublet–quartet equilibrium in the Co(PNP)Br_2 system[22,30] similar to that observed in **3**. In the current work, a key difference is the presence of two crystallographically distinct Co(II) complexes with different geometries.[52,53] Based on the structural evidence reported in the literature,[52,53] we expect that the Co(1) center (molecule A, τ_5 = 0.20), which has bond distances similar to the square planar **2**·EtOH, undergoes spin-crossover from high-spin S = 3/2 to low-spin S = 1/2, whereas the Co(2) center (molecule B, τ_5 = 0.08) remains high-spin over the entire temperature range.

We estimated the thermodynamic parameters of the putative spin crossover behavior of **3** by fitting the variable temperature $\chi_M T$ data to the ideal solution model.[54,55] In the most complete model, the two Co(II) complexes would have independently optimized g and temperature-independent magnetic susceptibility (TIP) values, which could be different in the low- and high-spin states (LS and HS, respectively). In addition, axial and rhombic magnetic anisotropy terms (D and E, respectively) should be present for Co(II) ions in the HS state. Assuming that one Co(II) ion, Co(1), undergoes spin crossover, and the other, Co(2), is HS at all temperatures, we identify ten variables that could be estimated: $g_{HS(Co2)}$, $g_{HS(Co1)}$, $g_{LS(Co1)}$, $TIP_{HS(Co2)}$, $TIP_{HS(Co1)}$, $TIP_{LS(Co1)}$, ΔH, T_C, $D_{(Co2)}$ and $E_{(Co2)}$. Since a model that contained all these variables would be

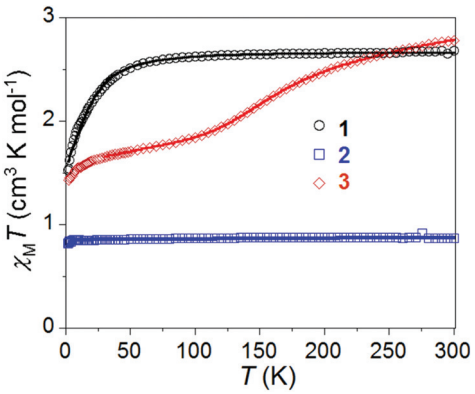

Fig. 5 Temperature dependence of $\chi_M T$ collected for solvated compounds **1**–**3** between 1.8 and 300 K. Data for **1**·0.25CH_2Cl_2 and **3** are measured at 1000 Oe, while data for **2**·EtOH are measured at 5000 Oe. Solid lines are fits to the data using the program PHI (detail in text) for compound **1**·0.25CH_2Cl_2 and **2**·EtOH. The solid red line is the fit to the data of **3** as described in the text (and as Model 2 in the ESI†).

overparameterized, we considered several different constraints for the g and TIP values of the HS and spin crossover Co(II) centers. For all models, we also neglected low-temperature data where magnetic anisotropy effects are prominent. These assumptions and corresponding effects on the model are detailed in the ESI.†

The model which provides the best fit to the data (Model 2, Fig. 5 and S7†) is based on the following equation:

$$\chi_M T = \frac{\left[\frac{{g_{HS}}^2}{4} C_{HS} + \frac{TIP_{HS}}{2} \times T\right] - \left[\frac{{g_{LS}}^2}{8} C_{LS} + \frac{TIP_{LS}}{2} \times T\right]}{1 + \exp\left[\frac{\Delta H}{R} \times \left(\frac{1}{T} - \frac{1}{T_C}\right)\right]} + \left[\frac{{g_{LS}}^2}{8} C_{LS} + \frac{TIP_{LS}}{2} \times T\right]$$

where g, C and TIP are the Landé factor, Curie constant and temperature-independent paramagnetism terms of the $S = 3/2$ (HS), and $S = 1/2$ (LS) states, respectively; R is the gas constant; ΔH is the enthalpy term; and T_C is the spin-transition temperature (where HS : LS = 50 : 50). Here, both Co(1) and Co(2) are high spin at 300 K, but only 50% of cobalt centers are doing spin crossover, therefore at T_C (= $T_{1/2}$) only 1/4 of the cobalt ions are LS.

The best fit of the data between 25 and 300 K (R = 0.99999) extracts g_{HS} = 2.200(1), g_{LS} = 2.90(5), TIP_{HS} = 0.0018(4) cm^3 mol^{-1}, and TIP_{LS} = 0.0024(2) cm^3 mol^{-1}. The g values found are reasonable for Co(II) ions in 5-coordinate geometries.[22,52,53] The thermodynamic parameters associated with the spin crossover event in compound **3** are as follows: T_C = 166(1) K, ΔH = 7.71(9) kJ mol^{-1} ΔS = 46.4(5) J K^{-1} mol^{-1}. The entropy term (ΔS) is larger than found in Co(II)-terpyridine based spin crossover complexes, but comparable to other long alkyl chain substituted-terpyridine based Co(II) spin crossover complexes.[56] The overall agreement between model and data supports the notion that spin crossover is operative in half of the Co(II) complexes.

Investigation of the field dependence of the magnetization measured at 2 K between 0 and 5 T (Fig. S5†) allows us to confirm the spin ground state for these Co(II) complexes. All three compounds give magnetization values close to saturation at 5 T. The magnetization for the square planar complex **2** saturates at 1.39μ_B at 5 T, consistent with an $S = 1/2$ system having a large g value. The M *vs.* H data (at 2 K in field range 0–5 T) are modeled well by a Brillouin function for a non-interacting isotropic $S = 1/2$ spin (Fig. 6) with a fit g value of 2.94(6), comparable to the value obtained from the susceptibility data. Compounds **1**·0.25CH_2Cl_2 and **3** show magnetizations of 2.27μ_B and 1.95μ_B, lower than expected for isotropic spin systems containing full and 50% occupancy of high-spin Co(II) ions, respectively (3.58μ_B for **1**·0.25CH_2Cl_2 and 2.42μ_B for **3**, assuming g values determined from susceptibility data); however, the depression of magnitude of magnetization is a common result of magnetic anisotropy contribution of the high-spin Co(II) centers. The non-superimposable isofield plots in the M *vs.* H/T data for compound **1**·0.25CH_2Cl_2, collected between 2 K and 20 K, confirms the presence of magnetic anisotropy (Fig. 6 inset). Best fits to these reduced magnetization data for **1**·0.25CH_2Cl_2, using the program ANISOFIT 2.0,[57] show significant axial (D) and rhombic (E) magnetic anisotropies, with D = −20.85 cm^{-1} and E = 3.82 cm^{-1} ($|E/D|$ = 0.183) which are comparable to the anisotropic parameters obtained from the fit of $\chi_M T$ *vs.* T data using PHI (Fig. 5).

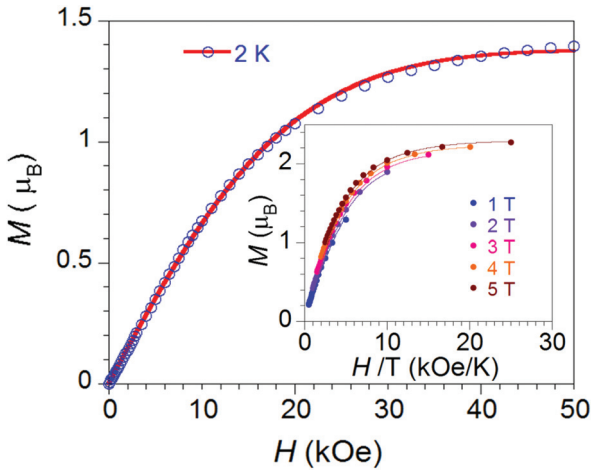

Fig. 6 Field dependence of magnetization for compound **1**·0.25CH_2Cl_2, collected at 2 K. The blue circles are the experimental data and the solid red line is the best fit to the Brillouin for non-interacting S = 1/2 spins with g = 2.94(6). Inset: M *vs.* H/T curves for **1**·0.25CH_2Cl_2; lines are of best-fit determined using ANISOFIT 2.0.

Conclusions

The pincer ligands (P^EN^EP, E = C, N, O) used in this study were selected because they are structurally similar and represent a synthetically accessible means to progressively alter the ligand field strength around Co(II) ions. While the expected ligand electronic effects are confirmed by cyclic voltammetry of complexes, structural characterization of **1–3** demonstrate that each ligand enforces unique geometries at the Co(II) in the solid state. These resulting changes in geometry govern the overall magnetic behavior of the Co(II) complexes.

Compound **2** is shown by X-ray crystallographic analysis to have a square planar geometry, with only one bromide anion bound to the Co(II) and the second in the outer coordination sphere. The magnetic properties are consistent with a low spin Co(II) ion throughout the temperature range examined.

In contrast, compounds **1** and **3** are 5-coordinate compounds in the solid state, with the pincer and two bromide anions in the primary coordination sphere. Depending on the solvent, the bromide anions can dissociate to form the 4-coordinate compound or a solvato-complex, which may play a role in the ability of these complexes to mediate inner-sphere reactivity. The magnetic properties for both compounds indicate that doublet and quartet states are energetically close to each other. The solid state magnetic properties of **3** indicate

spin-crossover behavior of half of the Co(II) ions; this analysis was complicated by the existence of two geometric isomers observed in the solid state, each of which appear to have unique magnetic properties. Notwithstanding, both **1**·0.25CH_2Cl_2 and **3** show magnetic anisotropy, which indicate the potential for single-molecule magnetism, which is currently being explored.

The electronic spin state of transition metal complexes plays an important role in rationalizing and imparting reactivity. This study on a series of catalytically relevant cobalt pincer complexes has important implications on how ligand changes intended to adjust the ligand field strength while maintaining the general structure can generate surprising effects on the geometry and coordination around the Co(II) ion. Specifically, the NH linker in compound **2** enforces a square planar geometry in the solid state instead of the 5-coordinate geometry observed for compounds **1** and **3**. Our study indicates these alternations in coordination geometry among structurally similar pincer ligands ultimately play the largest role in the magnetic properties of each compound, resulting in a Co(II) ions with low-spin, high-spin, and spin-crossover electronic behaviours.

Acknowledgements

This material is based upon work supported by the National Science Foundation under Grants CHE-1554744 (JYY, DWS, CT, & BNL) and CHE-1363274 (MPS & IB).

Notes and references

1 P. L. Holland, *Acc. Chem. Res.*, 2008, **41**, 905–914.
2 S. C. Bart, E. Lobkovsky, E. Bill and P. J. Chirik, *J. Am. Chem. Soc.*, 2006, **128**, 5302–5303.
3 E. R. King and T. A. Betley, *Inorg. Chem.*, 2009, **48**, 2361–2363.
4 E. R. King, E. T. Hennessy and T. A. Betley, *J. Am. Chem. Soc.*, 2011, **133**, 4917–4923.
5 D. A. Iovan and T. A. Betley, *J. Am. Chem. Soc.*, 2016, **138**, 1983–1993.
6 E. T. Hennessy and T. A. Betley, *Science*, 2013, **340**, 591–595.
7 E. T. Hennessy, R. Y. Liu, D. A. Iovan, R. A. Duncan and T. A. Betley, *Chem. Sci.*, 2014, **5**, 1526–1532.
8 O. Sato, J. Tao and Y.-Z. Zhang, *Angew. Chem., Int. Ed.*, 2007, **46**, 2152–2187.
9 M. A. Halcrow, *Spin-Crossover Materials: Properties and Applications*, Wiley, 2013.
10 E. R. King, G. T. Sazama and T. A. Betley, *J. Am. Chem. Soc.*, 2012, **134**, 17858–17861.
11 A. C. Bowman, C. Milsmann, E. Bill, Z. R. Turner, E. Lobkovsky, S. DeBeer, K. Wieghardt and P. J. Chirik, *J. Am. Chem. Soc.*, 2011, **133**, 17353–17369.
12 P. Gütlich, *Eur. J. Inorg. Chem.*, 2013, **2013**, 581–591.
13 A. B. Gaspar, M. Seredyuk and P. Gütlich, *J. Mol. Struct.*, 2009, **924–926**, 9–19.
14 P. Gütlich, A. B. Gaspar and Y. Garcia, *Beilstein J. Org. Chem.*, 2013, **9**, 342–391.
15 M. Nihei, T. Shiga, Y. Maeda and H. Oshio, *Coord. Chem. Rev.*, 2007, **251**, 2606–2621.
16 S. V. Larionov, *Russ. J. Coord. Chem.*, 2008, **34**, 237–250.
17 I. Krivokapic, M. Zerara, M. L. Daku, A. Vargas, C. Enachescu, C. Ambrus, P. Tregenna-Piggott, N. Amstutz, E. Krausz and A. Hauser, *Coord. Chem. Rev.*, 2007, **251**, 364–378.
18 H. A. Goodwin, in *Spin Crossover in Transition Metal Compounds II*, Springer Berlin Heidelberg, Berlin, Heidelberg, 2004, pp. 23–47.
19 S. Hayami, M. Nakaya, H. Ohmagari, A. S. Alao, M. Nakamura, R. Ohtani, R. Yamaguchi, T. Kuroda-Sowa and J. K. Clegg, *Dalton Trans.*, 2015, **44**, 9345–9348.
20 Y. Guo, X.-L. Yang, R.-J. Wei, L.-S. Zheng and J. Tao, *Inorg. Chem.*, 2015, **54**, 7670–7672.
21 F. Shen, W. Huang, D. Wu, Z. Zheng, X.-C. Huang and O. Sato, *Inorg. Chem.*, 2016, **55**, 902–908.
22 L. Sacconi, *Coord. Chem. Rev.*, 1972, **8**, 351–367.
23 W. S. J. Kelly, G. H. Ford and S. M. Nelson, *J. Chem. Soc. A*, 1971, 388–396.
24 W. V. Dahlhoff and S. M. Nelson, *J. Chem. Soc. A*, 1971, 2184–2190.
25 S. P. Semproni, C. C. Hojilla Atienza and P. J. Chirik, *Chem. Sci.*, 2014, **5**, 1956–1960.
26 J. V. Obligacion, S. P. Semproni and P. J. Chirik, *J. Am. Chem. Soc.*, 2014, **136**, 4133–4136.
27 G. Müller, M. Klinga, M. Leskelä and B. Rieger, *Z. Anorg. Allg. Chem.*, 2002, **628**, 2839–2846.
28 L. Chen, P. Ai, J. Gu, S. Jie and B.-G. Li, *J. Organomet. Chem.*, 2012, **716**, 55–61.
29 D. W. Shaffer, S. I. Johnson, A. L. Rheingold, J. W. Ziller, W. A. Goddard, R. J. Nielsen and J. Y. Yang, *Inorg. Chem.*, 2014, **53**, 13031–13041.
30 S. M. Nelson and W. S. J. Kelly, *J. Chem. Soc. D*, 1969, 94–94.
31 M. Kawatsura and J. F. Hartwig, *Organometallics*, 2001, **20**, 1960–1964.
32 D. Benito-Garagorri, E. Becker, J. Wiedermann, W. Lackner, M. Pollak, K. Mereiter, J. Kisala and K. Kirchner, *Organometallics*, 2006, **25**, 1900–1913.
33 W. H. Bernskoetter, S. K. Hanson, S. K. Buzak, Z. Davis, P. S. White, R. Swartz, K. I. Goldberg and M. Brookhart, *J. Am. Chem. Soc.*, 2009, **131**, 8603–8613.
34 E. Khaskin, Y. Diskin-Posner, L. Weiner, G. Leitus and D. Milstein, *J. Chem. Soc., Chem. Commun.*, 2013, **49**, 2771–2773.
35 P. Giannoccaro, G. Vasapollo, C. F. Nobile and A. Sacco, *Inorg. Chim. Acta*, 1982, **61**, 69–75.
36 A. D. Smith, A. Saini, L. M. Singer, N. Phadke and M. Findlater, *Polyhedron*, 2016, **114**, 286–291.

37 A. W. Addison, T. N. Rao, J. Reedijk, J. van Rijn and G. C. Verschoor, *J. Chem. Soc., Dalton Trans.*, 1984, 1349–1356.
38 A. P. Bashall, S. W. A. Bligh, A. J. Edwards, M. McPartlin, V. C. Gibson and O. B. Robinson, *Angew. Chem., Int. Ed. Engl.*, 1992, **31**, 1607–1609.
39 S. P. Semproni, C. Milsmann and P. J. Chirik, *J. Am. Chem. Soc.*, 2014, **136**, 9211–9224.
40 C. Lescot, S. Savourey, P. Thuéry, G. Lefèvre, J.-C. Berthet and T. Cantat, *C. R. Chim.*, 2016, **19**, 57–70.
41 M. Atanasov, D. Aravena, E. Suturina, E. Bill, D. Maganas and F. Neese, *Coord. Chem. Rev.*, 2015, **289–290**, 177–214.
42 F. E. Mabbs and D. J. Machin, *Magnetism and Transition Metal Complexes*, Dover Publications, 2008.
43 S. A. Carabineiro, L. C. Silva, P. T. Gomes, L. C. J. Pereira, L. F. Veiros, S. I. Pascu, M. T. Duarte, S. Namorado and R. T. Henriques, *Inorg. Chem.*, 2007, **46**, 6880–6890.
44 M. Cibian and G. S. Hanan, *Chem. – Eur. J.*, 2015, **21**, 9474–9481.
45 M. Cibian, S. Langis-Barsetti, F. G. De Mendonça, S. Touaibia, S. Derossi, D. Spasyuk and G. S. Hanan, *Eur. J. Inorg. Chem.*, 2015, **2015**, 73–82.
46 S. A. Cantalupo, S. R. Fiedler, M. P. Shores, A. L. Rheingold and L. H. Doerrer, *Angew. Chem., Int. Ed.*, 2012, **51**, 1000–1005.
47 N. F. Chilton, R. P. Anderson, L. D. Turner, A. Soncini and K. S. Murray, *J. Comput. Chem.*, 2013, **34**, 1164–1175.
48 T. Jurca, A. Farghal, P.-H. Lin, I. Korobkov, M. Murugesu and D. S. Richeson, *J. Am. Chem. Soc.*, 2011, **133**, 15814–15817.
49 J. M. Frost, K. L. M. Harriman and M. Murugesu, *Chem. Sci.*, 2016, **7**, 2470–2491.
50 G. A. Craig and M. Murrie, *Chem. Soc. Rev.*, 2015, **44**, 2135–2147.
51 L. Sacconi, *J. Chem. Soc. A*, 1970, 248–256.
52 A. B. Orlandini, C. Calabresi, C. A. Ghilardi, P. L. Orioli and L. Sacconi, *J. Chem. Soc., Dalton Trans.*, 1973, 1383–1388.
53 D. Gatteschi, C. A. Ghilardi, A. Orlandini and L. Sacconi, *Inorg. Chem.*, 1978, **17**, 3023–3026.
54 J. F. Berry, F. A. Cotton, T. Lu and C. A. Murillo, *Inorg. Chem.*, 2003, **42**, 4425–4430.
55 O. Kahn, *Molecular magnetism*, VCH, 1993.
56 S. Hayami, K. Murata, D. Urakami, Y. Kojima, M. Akita and K. Inoue, *Chem. Commun.*, 2008, 6510–6512.
57 M. P. Shores, J. J. Sokol and J. R. Long, *J. Am. Chem. Soc.*, 2002, **124**, 2279–2292.